ICSV 17
THE 17th INTERNATIONAL CONGRESS ON SOUND & VIBRATION
CAIRO 18 - 22 JULY, 2010

EXPERIMENTAL AND FINITE ELEMENT MODELS OF AN ADAPTIVE MAGNETORHEOLOGICAL SANDWICH BEAM

Peter L. Bishay[1], Mohammad Tawfik[2], and Hani M. Negm[3]

[1] *Teaching Assistant, Aerospace Engineering Department, Cairo University*
e-mail: peter_bishay@hotmail.com

[2] *Assistant Professor, Aerospace Engineering Department, Cairo University*
e-mail: mohammad.tawfik@gmail.com

[3] *Professor Emeritus, Aerospace Engineering Department, Cairo University*

The Magnetorheological fluid, as one of the smart materials, is the focus of many researches running nowadays and is getting to replace many materials in several commercial applications. This fluid is characterized by its ability to change from liquid into solid gel in few milliseconds as a result of applying a magnetic field.

This paper deals with a magnetorheological fluid embedded in an Aluminum sandwich beam to give the whole sandwich structure relevant controllability of various dynamic parameters such as natural frequencies, vibration amplitudes, and damping factors.

The test MR sandwich beam was manufactured and tested experimentally with several Magnetic field levels. The experimental results are then compared with the finite element model results for various magnetic field levels. The finite element model which is derived here for the first time is the most suitable model for dealing with sandwich beam problems with its various parameters.

1. Introduction

Magnetorheological (MR) fluids belong to the class of controllable fluids. The essential characteristic of MR fluids is their ability to reversibly change from free-flowing, linear viscous liquids to semi-solids having controllable yield strength in milliseconds when exposed to a magnetic field. This yield stress increases with the applied magnetic field. This feature provides simple, quiet, and rapid response interfaces between electronic controls and mechanical systems [1].

These fluids are suspensions of micron-sized magnetic particles in an appropriate carrier liquid. There are different types of liquids which can be used as the carrier fluid i.e. hydrocarbon oils, mineral oils and silicon oils. Normally, MR fluids are free flowing liquids having a consistency similar to that of motor oil. However, in the presence of an applied magnetic field, the iron particles acquire a dipole moment aligned with the external field which causes particles to form linear chains parallel to the field. This phenomenon can solidify the suspended iron particles and restrict the fluid movement.

1.1 Applications of MR fluids in adaptive sandwich beam structures

Typically, MR adaptive structures are achieved by having MR material layers placed between solid metal or composite layers as shown in Figure 1.1. The dynamic response of the structure can be varied when different levels of magnetic field are applied over the MR layer, which in turn produces structures with variable stiffness and damping properties. These variations in the rheological properties of MR materials are fast (a few milliseconds) and reversible, in response to variations in applied magnetic field, and can manipulate the dynamic vibration responses of the composite quickly. By controlling the applied magnetic field, the vibration of adaptive structures can be minimized for a broad range of external excitation frequencies.

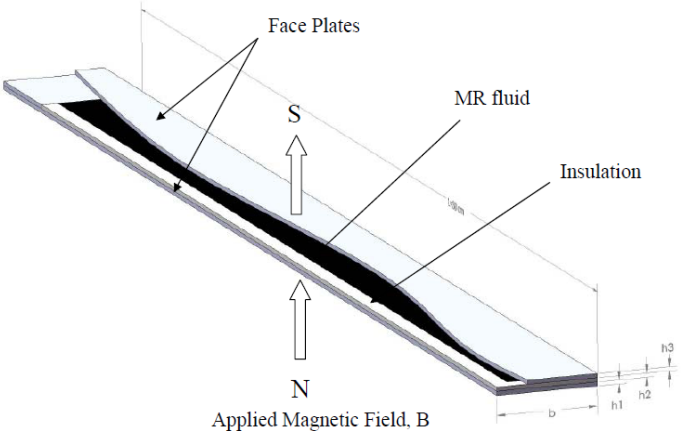

Figure 1.1: Three-layered adaptive beam configuration with MR material situated in the middle layer

Yalcintas [2] turned to the MR sandwich beam problem after making a performance comparison between ER (Electrorheological) and MR sandwich beams. From that study it was observed that both ER and MR adaptive structures show variations in their vibration responses when subjected to electric field and magnetic field respectively. These variations were mainly a decrease in vibration amplitudes and loss factors, and an increase in the natural frequency when the electric/magnetic field is increased. However, variations were more significant for MR adaptive structures than for the ER adaptive structures.

Yalcintas and Dai [3], followed by Sun *et al.* [4], developed a theoretical model for the MR sandwich beam based on Hamilton's principle and solved it for the case of Simply Supported beams to predict its vibration response. In addition, an MR adaptive beam structure was fabricated and tested in real time, and results were compared with the theoretical predictions.

Recently, V Lara-Prieto *et al.* [5] fabricated MR beams with two different materials for comparison purposes. Diverse excitation methods were considered as well as a range of magnetic field intensities and configurations. Controllability of the beam's vibration response was observed in the form of variations in vibration amplitudes and shifts in magnitudes of the resonant natural frequencies.

In this paper, the modelling of a Magnetorhelolgical (MR) sandwich beam structure using a higher order finite element method is presented for the first time. The computational results of the MR cantilever sandwich beam are compared with our experimental MR sandwich beam test results.

1.2 MR material rheological properties

According to MR rheological studies, the shear stress–shear strain relation is analyzed in two regimes as pre-yield and post-yield regimes. These behaviours are illustrated in Figure 1.2

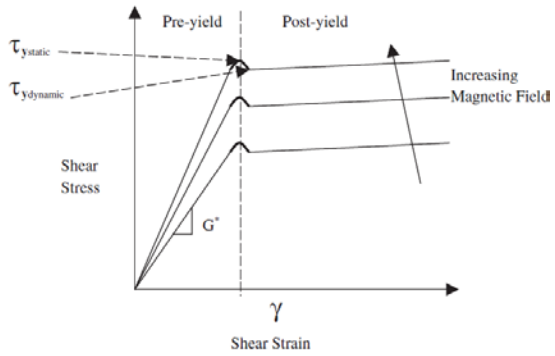

Figure 1.2: Shear stress –shear strain relationship for MR materials

In the earlier studies, the MR pre-yield regime was modelled by a linear viscoelastic model, and the post-yield regime was modelled by the Bingham plastic model. Li *et al.* [6] verified, through step-strain experiments, that the MR pre-yield behaviour is linearly viscoelastic up to 0.1% shear strain, and nonlinear above the 0.1% shear strain.

In the three-layered sandwich beam configuration, the MR materials experience shear stress and shear strain that is confined in the pre-yield regime. Yalcintas [7] determined that the shear strain experienced by the MR layer is then below 0.1%. Therefore, the linear viscoelastic theory is valid for the three-layered MR sandwich beam structure.

2. Finite Element modelling of the Three-Layer sandwich beam

In the following analysis we shall use Mead and Markus (MM) assumptions [8]:

- The transverse displacement (w) is the same for all the three layers.
- Rotary inertia and shear deformations in the upper and lower elastic layer beams are negligible.
- The Core layer has negligible bending stiffness and is subjected only to shear given by $\gamma = \frac{\partial w}{\partial x} + \frac{\partial u}{\partial z}$
- Linear theories of elasticity and viscoelasticity are valid.
- No slip occurs between the layers, and there is perfect continuity at the interface.
- All displacements are small.

The beam deformations are shown in Figure 2.1. A fundamental assumption of the approach is that line B-C in the core layer remains straight after deformation, as shown by line B'-C' in Figure 2.1. This, in effect, defines the axial displacement of any material position (x) inside the core as a linear interpolation of the displacements u_1' and u_3' at the surfaces of the face-sheets.

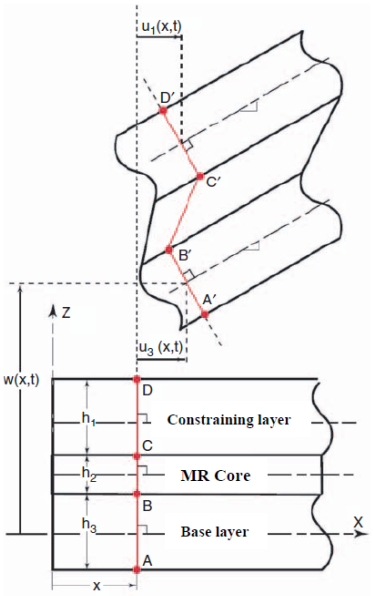

Figure 2.1: The undeformed (dashed line) and the deformed (Solid line) configurations of a three-layer sandwich beam under lateral loading

It can be proved that the axial displacement and the shear strain of the MR layer are given by [9]:

$$u_2 = \frac{u_1+u_3}{2} + \frac{h_1-h_3}{4}\frac{\partial w}{\partial x} \tag{1}$$

$$\gamma_{zx} = \frac{u_3-u_1}{h_2} + \frac{d}{h_2}\frac{\partial w}{\partial x} \tag{2}$$

where $d = \frac{h_1}{2} + h_2 + \frac{h_3}{2}$ is the distance between the reference lines of the undeformed face-sheets.

Since the beam is assumed not subjected to longitudinal loading, the resultant of the longitudinal normal forces must vanish, i.e.,

$$E_1A_1\frac{\partial u_1}{\partial x} + E_3A_3\frac{\partial u_3}{\partial x} = 0 \tag{3}$$

Integrating with respect to x and expressing u_3 in terms of u_1, we have

$$u_3 = -eu_1 \tag{4}$$

where $e = \frac{E_1A_1}{E_3A_3}$

Hence,

$$u_2 = \frac{(1-e)}{2}u_1 + \frac{(h_3-h_1)}{4}\frac{\partial w}{\partial x} \tag{5}$$

and

$$\gamma_{zx} = -\frac{(1+e)}{h_2}u_1 + \frac{d}{h_2}\left(\frac{\partial w}{\partial x}\right) \tag{6}$$

For simplicity, we will use "u" instead of "u_1".

2.1 Development of the equations of motion

The equations of motion in this investigation are developed using *Hamilton's principle*:

$$\delta\left(\int_{t1}^{t2}(T-U-V)dt\right) = 0 \tag{7}$$

where T is the kinetic energy, U is the strain energy, and V is the work done by external forces.

By taking the first variation, then integrating by parts with respect to time (t_1 and t_2 are arbitrary), we get the weak form of Hamilton's principle, which is used for deriving the finite element equations of the system.

In order to compare the experimental results with the computational ones we must take into consideration the presence of an Aluminium frame in the mid-layer that acts as a spacer and sealant for the MR fluid in the test sandwich beam.

The actual cross-section of the sandwich structure is as shown in Figure 2.2

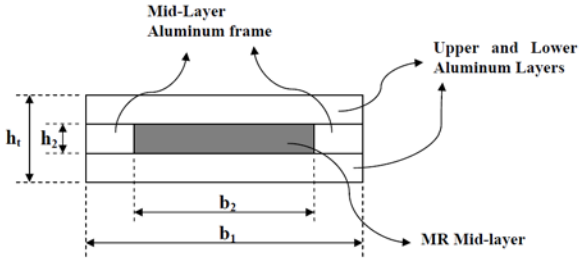

Figure 2.2: The real cross section for both the experimental test sandwich beam and the finite element model

We may write the total strain and kinetic energies of the MR sandwich beam for similar upper and lower layers as:

$$U = \frac{1}{2}E_1A_1\int_0^L\left(\frac{\partial u}{\partial x}\right)^2 dx + \frac{1}{2}E_1I_1\int_0^L\left(\frac{\partial^2 w}{\partial x^2}\right)^2 dx + \frac{1}{2}G_2A_2\int_0^L[-\frac{2}{h_2}u + \frac{d}{h_2}(\frac{\partial w}{\partial x})]^2 dx \quad (8)$$

$$T = \frac{1}{2}\rho_1A_1\int_0^L\left(\frac{\partial u}{\partial t}\right)^2 dx + \frac{1}{2}(\rho_1A_1 + \rho_2A_2)\int_0^L\left(\frac{\partial w}{\partial t}\right)^2 dx \quad (9)$$

where $A_1 = b_1h_t - b_2h_2$, $A_2 = b_2h_2$, $I_1 = \frac{b_1{h_t}^3}{12} - \frac{b_2{h_2}^3}{12}$, and $d = 2 \times h_2$

ρ_1 and E_1 are the density and the modulus of elasticity of the elastic layers (Aluminium), while ρ_2 is the density of the MR core layer and G_2 is its complex shear modulus, given for the used MR fluid by:

$$G_2(B) = G'(B) + G"(B)\,i \quad (10)$$

where: $G'(B) = 3.11 \times 10^{-7}B^2 + 3.56 \times 10^{-4}\,B + 5.78 \times 10^{-1}$,

$G"(B) = 3.47 \times 10^{-9}B^2 + 3.85 \times 10^{-6}B + 6.31 \times 10^{-3}$,(for Sun's model[4])

$$\text{Or, } G_2(B) = (1.25 \times 10^3 + i1.375 \times 10^1)B \quad (11)$$

with the value of G_2 with no applied magnetic field assumed as:

$$G_2(0) = (0.6125 + i0.0067375) \text{ MPa (for Yalcintas' model [3]).}$$

where B (Oersted) is the value of magnetic induction.

2.2 Finite Element Shape Functions

In this paper, different beam models are used with different numbers of nodes as shown in Figure 2.3. The interpolation functions used are regular polynomials.

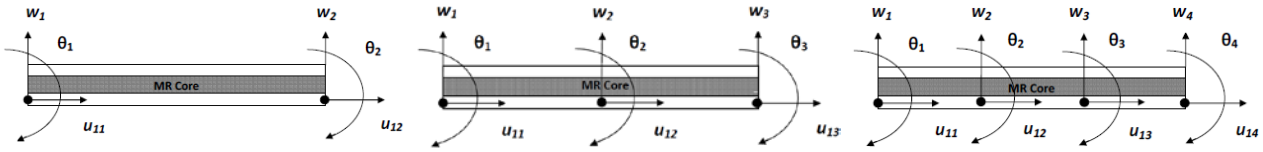

Figure 2.3: The proposed 2-node, 3-node, and 4-node sandwich beam elements with three degrees of freedom per node

The polynomial shape functions for the longitudinal displacement $u(x)$ and the transverse deflection $w(x)$ are:

$$u(x) = \sum_0^n a_ix^i \qquad 0 \le x \le L \quad (12)$$

$$w(x) = \sum_0^{2n} c_ix^i \qquad 0 \le x \le L \quad (13)$$

where n is the number of nodes in the element.

2.3 Finite element model

According to the normal procedure of the finite element method that could be found in any finite element textbook, we can rewrite the shape functions in the form:

$$u(x) = \lfloor N_u \rfloor\{\delta_u\} \quad (14)$$

$$w(x) = \lfloor N_w \rfloor \{\delta_w\} \tag{15}$$

where $\{\delta_u\} = \{u_1 \quad u_2 \quad \dots \quad u_n\}^T$

and $\{\delta_w\} = \{w_1 \quad \theta_1 \quad w_2 \quad \theta_2 \quad \dots \quad w_n \quad \theta_n\}^T$

Thus the element matrices may be written as:

$$U = \frac{1}{2}\{\delta\}^T [K]\{\delta\} \tag{16}$$

where $[K] = [K^u] + [K^w] + [K^\gamma]$, $[K^u] = E_1 A_1 \int_0^L \{N_{u_x}\} \lfloor N_{u_x} \rfloor dx$,

$[K^w] = E_1 I_1 \int_0^L \{N_{w_{xx}}\} \lfloor N_{w_{xx}} \rfloor dx$, $[K^\gamma] = G_2 A_2 \int_0^L \{N_\gamma\} \lfloor N_\gamma \rfloor dx$

and $\lfloor N_\gamma \rfloor = [-\frac{2}{h_2} \lfloor N_u \rfloor + \frac{d}{h_2} \lfloor N_{w_x} \rfloor]$

$$T = \frac{1}{2}\{\delta\}^T [M]\{\delta\} \tag{17}$$

where $[M] = [M^u] + [M^w]$, $[M^u] = \rho_1 A_1 \int_0^L \{N_u\} \lfloor N_u \rfloor dx$,

$[M^w] = (\rho_1 A_1 + \rho_2 A_2) \int_0^L \{N_w\} \lfloor N_w \rfloor dx$

Finally, the element equation of motion becomes:

$$[M]\{\ddot{U}\} + [K]\{U\} = \{F\} \tag{18}$$

$\{F\}$ is the external load vector, and will be set to zero during the free vibration analysis.

A general MATLAB code for any-order element was developed to calculate the global mass and stiffness matrices for the MR sandwich beam, and hence calculate the natural frequencies and the loss factors for the MR sandwich beam for various beam boundary conditions. The code was verified by comparing its results with the published analytical results for the case of SS-SS MR sandwich beam. The finite element method showed high accuracy with only a small number of elements, especially when using the higher order elements.

3. Experimental Model

The MR fluid was manufactured according to the recipe of Dr. David Carlson [10]. This fluid has the maximum yield strength and magnetic properties that are similar to the Rheonetic™ MRF-122-2ED magnetorheological fluid produced commercially by Lord Corporation.

The sandwich beam was then manufactured; it is composed of upper and lower Aluminium layers and the MR fluid filled the mid-layer Aluminium cavity which acts as a spacer and sealant. The dimensions of the MR sandwich beam are as follows: 30 cm length, 2 cm width and 3 mm thickness (each layer is 1 mm thick). The MR fluid layer width is 12 mm because the mid-layer Aluminium frame width is 4 mm on each side of the MR fluid. The layers were adhered to each other using a high strength Epoxy adhesive, See Figure 3.1

Figure 3.1: Making the MR sandwich beam: the MR fluid filling the Mid-layer cavity

The sandwich beam was then clamped properly to a fixed stand on the test bed. The test bed was designed to prevent any external vibrations from reaching the test structure. Hence, the end support of the cantilever is necessarily a fixed end.

A stand that carries the permanent magnetic poles was designed and manufactured. The magnets stand allows for changing the distance between both the magnetic poles and the sandwich beam in order to change the magnetic field level.

The generated magnetic field from the permanent magnetic poles was measured using an American Gauss/Tesla meter "F.W. Bell" model 5080 for different distances between the magnetic poles.

Because the used transducers have significant height that would hinder the magnetic poles from approaching the MR sandwich beam, we selected a point 2 cm from the beam tip to attach the shaker and the force transducer. We also selected the beam tip to be the point where the accelerometer is attached. The tip thus shows the peak of the first natural frequency clearly in the frequency response plot.

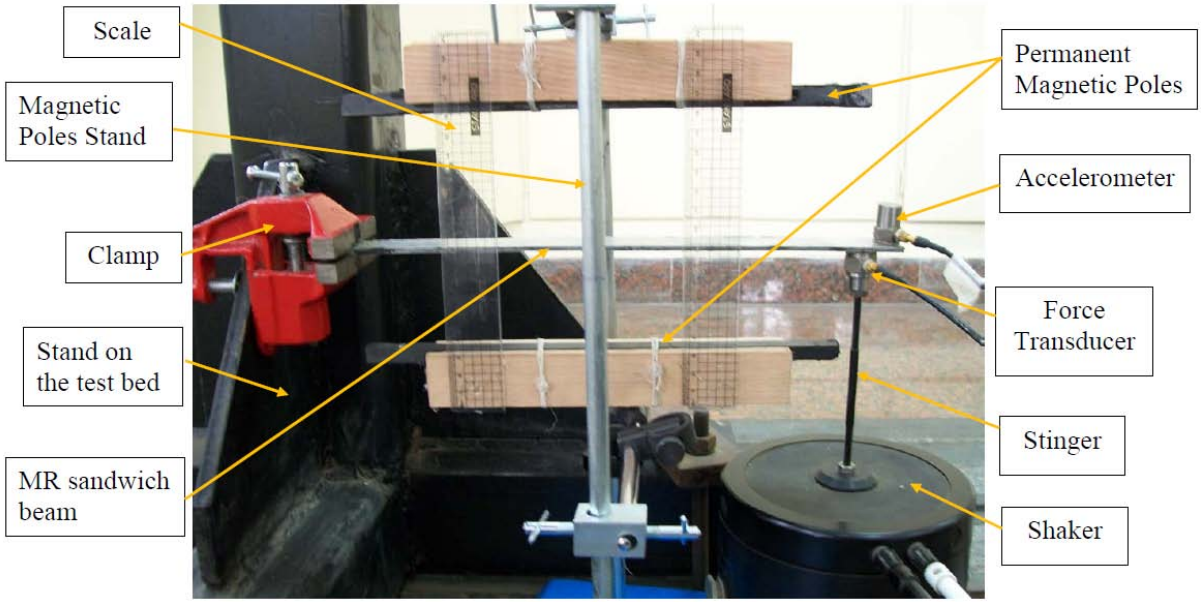

Figure 3.2: the whole test configuration

4. Comparison of results and Conclusions

The experimental MR sandwich beam test specimen was dynamically tested using Pseudo Random excitation which is a fast excitation technique, causes no leakage problems, and does not need any special kind of weighting. The test was done for no magnetic poles placed, 21 mm and 11 mm spacing between the magnetic poles. This corresponds to zero, 500 Gauss, 1000 Gauss magnetic field strengths. The frequency range of the test was 0-100 Hz. The measured FRFs were then transferred from a B&K 3550 Analyzer or Multichannel Analysis system to Test.Lab Modal Analysis software that could obtain the modal parameters (Mainly natural frequencies and loss factors) of the measured frequency response.

We also calculated the frequency response of the cantilevered MR sandwich beam using our MATLAB code with the proposed Finite element model after inserting all the problem's inputs. For the sake of accuracy, the results were obtained using 10 three-node elements.

The graphs in Figure 4.1 below show the first natural frequency for both the experimental and the computational finite element models for the three magnetic field cases. Table 4-1 gives the numerical values of the natural frequencies and the damping loss factors of both models.

It is seen that the Finite element model, which is based on the only available model for the MR fluid in the pre-yield region presented in [3] and [4], underestimates the damping loss factor of the MR sandwich beam. Second, it overestimates the natural frequency values with an applied magnetic field. This means that the used finite element model overestimates the stiffening effect and underestimates the damping effect of the MR fluid.

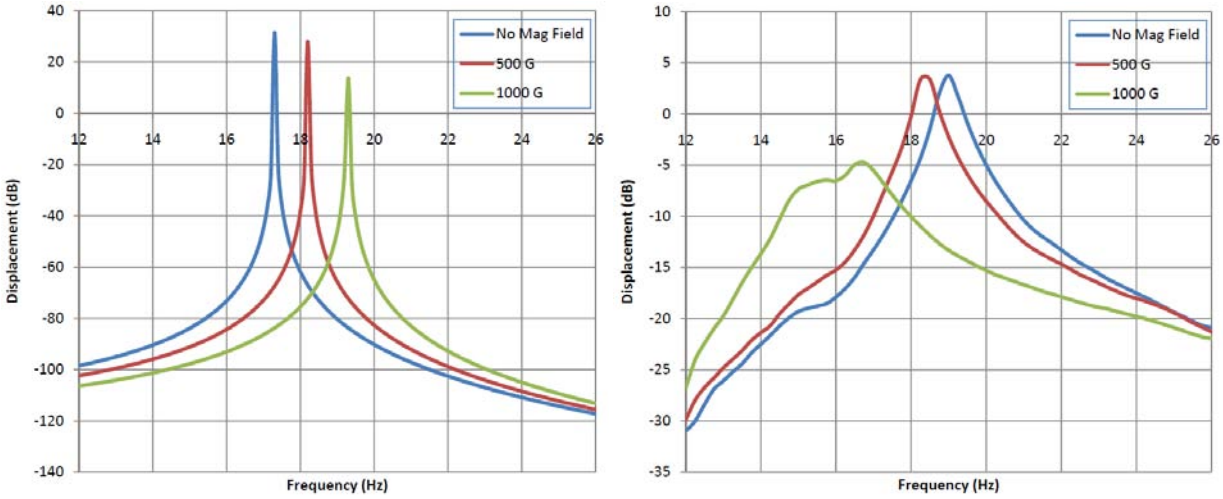

Figure 4.1: The first natural frequency of the MR sandwich beam (Left: FE model, Right: Experimental model)

Table 4-1: Comparison between the Experimental and FE models' results

	Finite Element Model		Experimental Model	
	1st Natural Freq. (Hz)	Damping Loss Factor	1st Natural Freq. (Hz)	Damping Loss Factor
No Mag. Field	17.3068	0. 290 %	19	5.26 %
500 Gauss	18.2077	0. 310 %	18.25	6.82 %
1000 Gauss	19.2859	0. 317 %	16.75	13 %

On the other hand, the above experimental results predict a decrease in the natural frequency as the applied magnetic field increases, which mean that the damping effect of the common MR fluid is higher than its stiffening effect. These experimental results are consistent with Lara-Prieto recent results [5].

This study reveals the need for more adequate modelling of the MR fluid which properly represents both its damping and stiffening effects.

REFERENCES

[1] G.Yang, *Large-Scale Magnetorheological Fluid Damper for Vibration Mitigation: Modeling, Testing and Control*, Ph.D dissertation, University of Notre Dame, 2001. http://cee.uiuc.edu/sstl/gyang2/ch2.pdf.

[2] Melek Yalcintas and Heming Dai, "Magnetorheological and Electrorheological Materials in Adaptive Structures and their Performance Comparison", *Smart Mater. Struct.* **8**, 560–573 (1999).

[3] Melek Yalcintas and Heming Dai, "Vibration Suppression Capabilities of Magnetorheological Materials Based Adaptive Structures", *Smart Mater. Struct.* **13,** 1–11 (2004).

[4] Qing Sun, Jin-Xiong Zhou, Ling Zhang, "An Adaptive Beam Model and Dynamic Characteristics of Magnetorheological Materials", *Journal of Sound and Vibration* **261,** 465–481 (2003).

[5] V. Lara-Prieto *et al*, "Vibration characteristics of MR cantilever sandwich beams: experimental study", *Smart Mater. Struct.* **19**, 015005 (2010).

[6] Li WH, Du H, Chen G, Yeo S H and Guo N Q, "Nonlinear Rheological Behavior of Magnetorheological Fluids: Step-Strain Experiments", *J. Smart Mater. Struct.* **11** 209–17 (2002).

[7] Melek Yalcintas, *An Analytical and Experimental Investigation of Electrorheological Material Based Adaptive Structures*, Dissertation Lehigh University, 1995.

[8] Mead D. J. and Markus S, "The forced vibration of a three layer damped sandwich beam with arbitrary boundary conditions", *Journal of Sound and Vibration* **10**, 163–175 (1969).

[9] Jalil Rezaeepazhand and Lotfollah Pahlavan, "Transient Response of Sandwich Beams with Electrorheological Core", *Journal of Intelligent Material Systems and Structures* **20**, 171-9 (2009).

[10] David Carlson, "Dr. Dave's do-it-yourself MR fluid, designing with MR fluid, magnetic circuit design", *Lord Corporation*, 2004.